euspen's 25th International Conference & Exhibition, Zaragoza, ES, June 2025
www.euspen.eu

Robot-ensemble for the Automated Production of High-Performance Metal Optics with In-Line Metrology

Ralf Steinkopf, Matthias Heinze, Tobias Herffurth, Gilbert Leibeling, Stefan Heist, Jan Kinast, Stefan Risse, Gunther Notni

Fraunhofer Institute for Applied Optics and Precision Engineering IOF Jena

ralf.steinkopf@iof.fraunhofer.de

Abstract
The manufacturing process of high-performance optics, utilized in applications from astronomical instruments to lithography tools, typically relies on production processes initially developed for small batch sizes and high quality. The growing demand for high-performance optics requires a transformation of these processes enabling high throughput cycles with scalable batches and even higher surface qualities. Considering this, the measurement technologies for these optics must also be re-evaluated. The state of the art includes local measurements with high resolution (e.g., Atomic Force Microscopy or White Light Interferometry) and global measurements with lower lateral resolution (e.g., interferometry), both realized in a separated measurement enviroμent. Instead, the measurement of large quantities of optics should be carried out in-situ and obtain high-resolution data for the entire surface within the production setup.
This article demonstrates how an ensemble of three robots equipped with polishing, cleaning and measuring tools, processes a batch of three metal mirrors, simultaneously. The polishing technique allows for surfaces roughness below 0.3 nm Sq and uses cleaning methods that enable in-situ measurements between the polishing steps.
Two different sensors provide high resolution data. High-Spatial Frequencies (HSF) and surface contamination are assessed using Angle-Resolved Scattering (ARS) measurements. Deflectometry is employed to inspect the surface for defects and measure Mid-Spatial Frequencies (MSF). The use of robots with interchangeable tools enables different processing configurations and straightforward scalability.

High-performance optics, Metal optics, In-situ measurements, Deflectometry, Scattering light measurements, Polishing, Cleaning

1. Introduction

The core of many groundbreaking technologies is based on optical systems. Lithographic applications for instance, continue to keep pace with Moore´s Law even 60 years after its initial proclamation [1]. Telescopes used in satellite communication and environmental observation also rely on highly accurate optics [2]. The quality of the optical elements achieves accuracies within a few nanometers, depending on advanced manufacturing technologies and metrology devices. However, since these technologies were not originally developed for high throughput rates, the recent demand requires a transformation of these processes. The paper presents a potential solution: a robot ensemble equipped with polishing and cleaning tools as well as metrology devices. This creates a highly flexible production cell, that can be scaled up for higher throughput and adapted for different tasks by changing the robot tools. The described process focuses on three parts of the process chain:

- Analyzing of High-Spatial Frequencies (HSF)
- Analyzing of Mid-Spatial Frequencies (MSF)
- Chemical-Mechanical Polishing (CMP) of HSF and MSF

The measurement and correction of Long-Spatial Frequencies (LSF) are excluded from this setup. However, Xiaolong Ke et al. [3] have demonstrated that LSF can be corrected in various ways using robot setups. Instead, the paper focuses on addressing the complex challenge of measuring and polishing high performance optics in the central regions of HSF and LSF, within the spatial frequency range of 1×10^{-1} µm^{-1} to 5×10^{-4} µm^{-1}. The relationship between HSF, MSF and LSF is not clearly defined within the scientific community [4]. This paper concentrates on a practical approach, defining LSF as those errors that can be corrected with deterministic processes such as Magneto-Rheological Finishing (MRF) or Ion-Beam Figuring (IBF) with spatial frequencies from 2×10^{-4} µm^{-1} to $(Ø/2)^{-1}$ µm^{-1} and HSF as those corrected using stochastic approaches like CMP with spatial frequencies of 1×10^{0} µm^{-1} to $0{,}4\times10^{-2}$ µm^{-1}. MSF are situated between the two and can be corrected, though with limitations, using both deterministic and stochastic methods. Different metrology devices are used to measure the specific spatial frequencies. High frequency errors are often measured using Atomic-Force Microscopy (AFM), while White-Light Interferometry (WLI) is a classical approach for measuring MSF [4]. However, both technologies measure relatively small spots compared to the optical surface and are not designed for scanning and analyzing the entire surface, which is standard for measuring LSF [5]. Given that most complex optics consist of aspheres or freeforms manufactured with sub-aperture tools, they are susceptible to HSF and MSF that are not uniformly distributed [6]. Consequently, spot measurements fail to provide complete information about the expected performance of the optical component. To address this problem, it is planned to use articulated robots to scan the complete surface. The HSF measurements will be conducted using Angle-Resolved Scattering (ARS) measurements, while MSF will be analyzed using deflectometry. The optical surface is polished by another articulated robot using CMP technology. An integrated cleaning tool prepares the surface after polishing for the next measurement. This process allows an iterative approach without removing the parts from the manufacturing environment, saving setup time, minimizing handling risk and facilitating high resolution measurements.

2. Process chain for the manufacturing of metal optics

Metal optics are an excellent choice for reflective systems. Applications spanning from Near-Infrared (NIR) to Infrared (IR) often utilize on directly diamond-machined Aluminium surfaces. This material provides a favorable combination of lightweight, stiffness and ductility. However, the crystalline structure of many metal alloys limits their application range due to high surface roughness. To mitigate this, functional layers of specialized materials are applied to the surface. Nickel Phosphorus (NiP) with its X-ray amorphous structure, is one such material. To avoid the bi-metallic effect in this material combination it is possible to adjust the thermal expansion coefficient of the Aluminium based substrate material [7]. Table 1 outlines the complete process chain for the manufacturing of high-performance metal optics used in applications ranging from the Visual (VIS) spectrum to the Extreme-Ultraviolet (EUV) spectrum. The initial steps in the process chain, pre-manufacturing and diamond machining, are not feasible for manufacturing with jointed-arm robots due to the low stiffness and repeatability of the robot kinematic.

Table 1 Process chain for the manufacturing of high performance metal optics and related measurement technologies

	Process step	**Measurement type**
1.	Pre-manufacturing Al	Outer dimensions
2.	Diamond machining Al	Optical surface (LSF)
3.	Electroless NiP – Plating	Outer dimensions
4.	Diamond machining NiP	Optical surface (LSF)
5.	Correction polishing NiP	Optical surface (LSF, MFS)
6.	Smoothing polishing NiP	Optical surface (MSF, HFS)

The soft contact zones of the polishing tools instead are well-suited for robot polishing. To demonstrate the effectiveness and scalability of the robot-operated polishing and measurement cell, a sample mirror was extracted from a telescope design [8] utilized in an early satellite constellation, that operated from 2009 to 2020. Three identical pieces of this mirror were premanufactured, diamond-machined and NiP plated. From the next process step onward (Table 1, process step 4), all three mirrors were mounted on a fixture and handled as a single inseparable batch. Figure 1**Fehler! Verweisquelle konnte nicht gefunden werden.** illustrates the manufacturing setup of this batch during diamond machining.

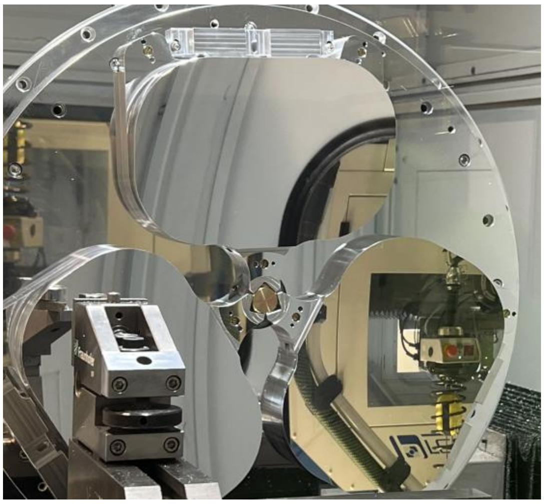

Figure 1 Manufacturing of three mirrors as one batch during diamond machining

3. Robot setup

The robot cell (see Figure 2), consisting of three Universal Robots (UR), is arranged to operate on parts of maximum Ø 500 mm. Each UR is equipped with one specialized tool:

- Polishing and cleaning tool
- Deflectometric detector
- ARS detector

The batch of mirrors is centered in the polishing setup within reach of all three UR. The following process sequence was implemented (Table 2):

Table 2 Process sequence for measuring, polishing and cleaning

#	**Process step**	**Process logic**
1.	Measurement: Within specification Measurement: Out of specification	Process completed Go to step 2
2.	Polishing	Go to step 3
3.	Cleaning	Go to step 1

This allows for an iterative process with variable abort criteria. The system can decide automatically if the process needs another polishing run or if the process time had been adequate and has to be terminated.

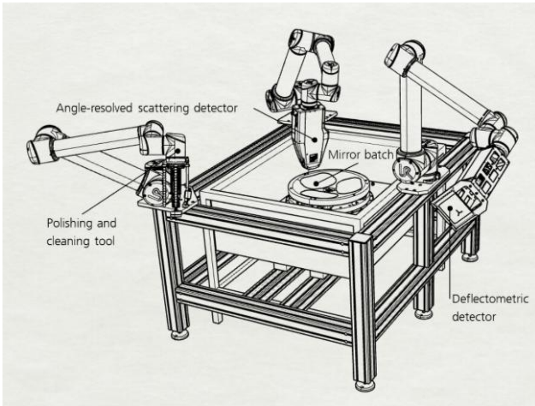

Figure 2 Robot ensemble prepared to process a batch of mirrors

In this demonstration, the tools are fixed on the UR. In real production, using interchangeable heads would be more efficient. Polishing time accounts for approximately 80 % of the total processing time. Employing three URs equipped with polishing tools that switch to metrology tools during measure cycles would significantly reduce processing time. While this could be achieved with commercially available interfaces, it was not included in the demonstration setup. Instead, the focus was on integrating metrology devices in the manufacturing environment.

4. Chemical-mechanical polishing and cleaning

Diamond machined Aluminium surfaces typically achieve HSF roughness of lower than 10 nm Sq and LSF errors of lower than 1 µm Sq, depending on size and geometry of the part.

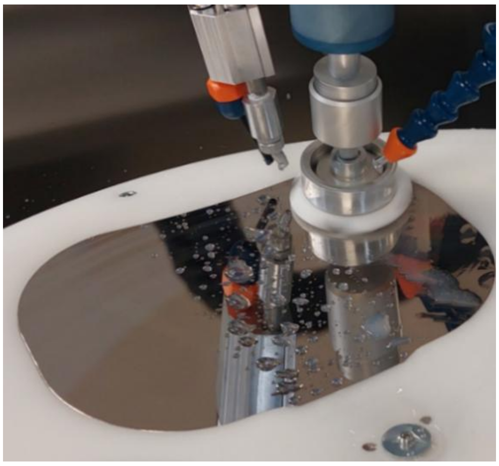

Figure 3 Polishing and cleaning tool during operation

Due to the use of sub-aperture tools, the process is susceptible to MSF errors, which lie between these two spatial ranges.
The already high quality of the diamond machined optical surface allows for direct polishing with colloidal slurries, composed of nanoparticles and a chemical component that softens the material during the polishing process. This combination, also known as CMP, effectively smooths optical surfaces to HSF roughness of lower than 0.3 nm Sq [9]. By varying the particle size of the slurry and the stiffness of the polishing tool, the cut-off frequency of the addressable error frequency can be adjusted and shifted from HFS to MSF correction. Consequently, incoming measurements from the ARS detector for HSF roughness and the deflectometry detector for MSF errors indicate the process parameter for the subsequent polishing step. The process parameters for the chosen configuration are available in the data base and selected accordingly. Following the polishing process, a cleaning and drying procedure is performed to prepare the optical surface for the measurement. The cleaning sequence begins with rinsing both, the tool and the surface with deionized water. The combined polishing and cleaning tool consist of a central polishing pad and a larger, more flexible cleaning pad at the edge. By programming the tool position during cleaning to be slightly higher than during polishing, the surface is effectively cleansed of sticky slurry residuals. This procedure is followed by another rinsing sequence and finished with a nitrogen flush.

5. Angle Resolved scattering measurement

HSF roughness on optical components contributes to scattering losses and stray light, which leads to a reduction in contrast. In comparison, features with low spatial frequencies impair the optical imaging quality, which is associated with classical aberrations and leads to a loss of resolution. MSF affects both, imaging quality and scattering, producing unique effects, often characterized by regular discrete orders. Consequently, by analyzing the ARS, HSF can be assessed and even measured [10].
A corresponding sensor device for calibrated ARS and HSF roughness measurements has been integrated into the combined setup.
This sensor concept is based on the approaches presented in [11] using a CMOS matrix detector for scattering detection. However, a novel implementation of this sensor provides advanced optional features such as refocusing to compensate for the sample curvature, a nitrogen nozzle for dust removal, and a microscope to correlate scattering and surface features such as defects and particles [12].
Figure 4 displays exemplary scattering results measured on the mirror after diamond machining (Table 1: process step 4, Figure 4: top) and polishing (Table 1: process step 6, Figure 4: bottom). The central part of the images corresponds to the specularly reflected beam, which is not analyzed and thus removed from the images. HSF information is captured in the scattering of the remaining areas. In these specific images, the sensitivity level of the sensor was set to emphasize the diffraction from periodic turning marks and the HSF structures in between the turning marks, all within a single measurement duration of less than <1 s. These features are visible as the scattering pattern on the diagonal line that is significantly reduced after the smoothing polishing. Hence, residual surface structures from diamond turning are removed. Furthermore, the HSF roughness calculated from scattering is reduced by a factor of more than three.

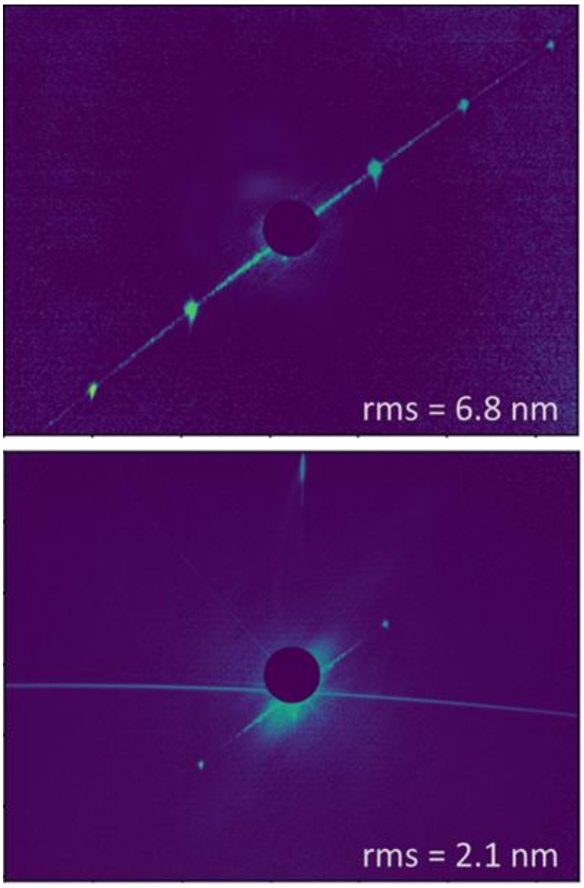

Figure 4 ARS distributions of the mirror (spot size app. Ø2 mm); Top: After diamond machining; Bottom: Reduced HSF after polishing

6. Deflectometry

MSF is inherent in most fabrication processes using sub-aperture tools, leaving regular pattern and machining marks. Accurately detecting MSF on high-performance optical surfaces is essential for ensuring optimal performance and quality control. This is achieved with an integrated high precision deflectometry sensor designed to meet this crucial metrology requirement.

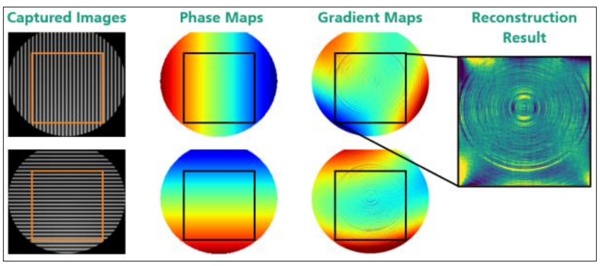

Figure 5 Structure-sensitive surface reconstruction workflow with captured orthogonal oriented fringe patterns

The sensor utilizes a novel data processing and surface reconstruction workflow to achieve nanometer-level precision in measuring MSF. The surface reconstruction is based on displayed fringe patterns which are observed by a camera via the reflective surface. To be sensitive to arbitrary oriented object structures, vertical and horizontal aligned fringe patterns are utilized as basis for the surface reconstruction. A novel optimization algorithm is applied to determine a virtual reference surface which is used for gradient based reconstruction (see Figure 5) [13].

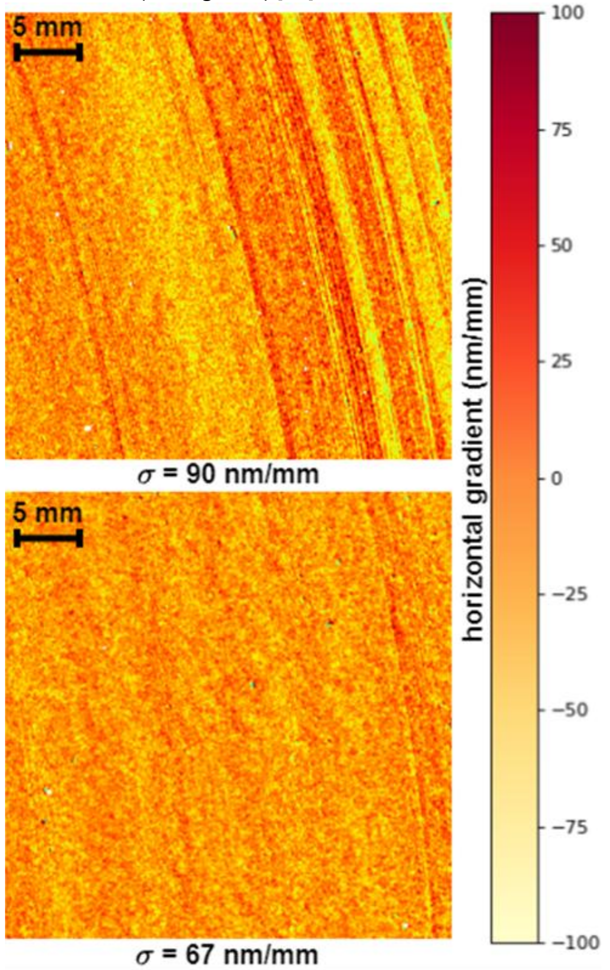

Figure 6 Horizontal surface gradient; Top: After diamond machining; Bottom: Reduced MSF after polishing

Figure 6 shows the horizontal surface gradient of the deviation between a sample and its reference. The data is calibrated by using measurement results obtained from the tactile profilometer UA3P. In the top image, the sensor captured a surface patch with a field of view of 40 x 40 mm ^{2}after diamond turning (Table 1, process step 4) in approximately 1 s, revealing dominant surface structures. The pattern is significantly reduced after CMP (Table 1, process step 6), as shown in the bottom image. The variance σ, as measure for the spread of the captured data points around their mean value, could be reduced by 25 %.

7. Summary

The demonstrated polishing cell with included metrology has demonstrated its capacity in processing large high-performance optics. Three single mirror substrates were polished, cleaned and measured within the production line, simultaneously (Figure 7). It could be demonstrated that the HSF roughness is analyzed with the ARS detector and subsequently reduced by a factor of three by CMP. Even so, the ARS detector will be optimized in future through the implementation of a shorter laser wavelength. It is envisaged to further increase the covered spatial frequency and the overall sensitivity to fully assess the roughness also for the super polished surfaces after CMP.

MSF was detected with the deflectometry sensor. The captured fringe pattern was used to reconstruct the surface and to visualize waviness on the surface. The CMP process significantly reduced the MSF by 25 %.

The interaction between metrology and polishing tools in a single setup enables the scaling of manufacturing processes based on batch sizes. Additionally, the removal of setup times between the correction cycles leads to higher throughput rates and increases the surface accuracy.

Figure 7 Robot ensemble during operation on a batch of mirrors

References

[1] Kaiser, W., “Evolvement of Lithography Optics Towards Advanced EUV Lithography”, IEEE ED-M 2 (2024).

[2] Flannigan, L. et al., “Mid-wave and long-wave infrared transmitters and detectors for optical satellite communications—a review”, J. Opt. 24 (2022).

[3] Ke, X. et al., “Review on robot-assisted polishing: status and future trends”, Robot. Comput.-Integr. Manuf. 80 (2023).

[4] Rolland, J. et al., “Freeform optics for imaging”, Optica 8 (2021).

[5] Sykora, D. M. and de Groot, P., “Instantaneous measurement Fizeau interferometer with high spatial resolution”, in *Proc. of SPIE* 8126 (2011).

[6] Han, Y. et al., “Analytical and stochastic modelling of surface topography in time-dependent sub-aperture processing”, Int. J. Mech. Sci. 175 (2020).

[7] Kinast, J. et al., “Thermal expansion coefficient analyses of electroless nickel with varying phosphorous concentrations”, Surf. Coat. Technol. 259 (2014).

[8] Risse, S. et al., “Novel TMA telescope based on ultra precise metal mirrors”, in *Proc. of SPIE* Vol. 7010 (2008).

[9] Porwol, T. et al., “Super-polished metallic freeform optics for EUV-application”, in *Proc. of SPIE* Vol. 12953 (2024).

[10] Herffurth, T. et al., "Comprehensive nanostructure and defect analysis using a simple 3D light-scatter sensor", Appl. Opt. 52 (2013).

[11] Herffurth, T. et al., "Assessing surface imperfections of freeforms using a robotic light scattering sensor", Opt. Eng. 58 (2019).

[12] Bergner, A. et al., "Roughness, particle, and defect analysis of freeform surfaces", in *Proc. of Optical Interference Coatings Conference* (2022).

[13] https://github.com/IOF-SWAP/swap-success -story